Vietnam Journal of Chemistry, International Edition, **55**(5): 657-662, 2017
DOI: 10.15625/2525-2321.2017-00525

Preparation and characterization of magnesium hydroxyapatite coatings on 316L stainless steel

Vo Thi Hanh[1,2*], Pham Thi Nam[3], Nguyen Thu Phuong[3], Nguyen Thi Thom[3], Le Thi Phuong Thao[2], Dinh Thi Mai Thanh[1,4]

[1]*Graduate University of Science and Technology, Vietnam Academy of Science and Technology*

[2]*Department of Chemistry, Basic Science Faculty, Hanoi University of Mining and Geology*

[3]*Institute for Tropical Technology, Vietnam Academy of Science and Technology*

[4]*University of Science and Technology of Hanoi, Vietnam Academy of Science and Technology*

Received 9 March 2017; Accepted for publication 20 October 2017

Abstract

Magnesium hydroxyapatite coatings (MgHAp) were deposited on the surface of 316L stainless steel (316L SS) substrates by electrodeposition technique. Different concentrations of Mg^{2+} ion were incorporated into the apatite structure by adding $Mg(NO_3)_2$ into electrolyte solution containing 3×10^{-2} M $Ca(NO_3)_2$, 1.8×10^{-2} M $NH_4H_2PO_4$ and 6×10^{-2} M $NaNO_3$. With Mg^{2+} concentration 1×10^{-3} M, the obtained coatings have 0.2 wt% Mg^{2+}. The influences of scanning potential ranges, scanning times to deposit MgHAp coatings were researched. The analytical results FTIR, SEM, X-ray, EDX, thickness and adhension strength showed that MgHAp coatings were single phase of HAp, fibrous shapes, thickness 8.1 µm and adhesion strength 7.20 MPa at the scanning potential ranges of 0÷-1.7 V/SCE and scanning times of 5 scans.

Keywords. 316L SS, Electrodeposition, MgHAp.

1. INTRODUCTION

Hydroxyapatite ($Ca_{10}(PO_4)_6(OH)_2$, HAp) is a main component in the mineral phase of natural bone, teeth and hard tissue. HAp is widely used in medical fields because it has high biocompatibility and chemical composition as the natural bone. HAp coating is covered on implant materials such as 316L stainless steel, titanium metal,... to improve the quality and biocompatibility. HAp could stimulate the bonding between the host bone to implant materials and make bone healing ability faster [1].

HAp coatings on metals or alloys were synthesized by many methods such as sol-gel [2], plasma spraying [3], electrophoretic deposition and electrodeposition [4] .... Among them, the electrodeposition method offers much advantages, such as low temperature, controlling the coating thickness, the high purity, high adhesion strength and low cost of the equipment [5].

Sodium has been detected as an abundant trace element in natural bone, sodium can enhance cell adhesion and bone metabolism [6]. Next to the presence of sodium, magnesium is a trace element indispensable in all skeletal metabolism stages, the formation of bone tissue [7], the stimulation of the osteoblast proliferation and bone strength structure [8]. Therefore, magnesium and sodium are incorporated into HAp in order to improve further mechanical properties and biological activity. In addition, the presence of Mg^{2+}, Na^+, and NO_3^- in the electrolyte solution could be increased the conductivity and the efficiency of the synthesis process by electrochemical method.

This paper introduces synthesis results of MgHAp coatings on 316L SS substrate in a solution containing Ca^{2+}, $H_2PO_4^-$, Na^+ and Mg^{2+} by cathodic scanning potential method with different of Mg^{2+} concentrations, scanning potential ranges and scanning times.

2. EXPERIMENTAL

2.1. Preparation of MgHAp coatings

316L SS (size of 100×10×2 mm, composed of 0.27 % Al; 0.17 % Mn; 0.56 % Si; 17.98 % Cr; 9.34 % Ni; 2.15 % Mo; 0.045 % P; 0.035 % S and 69.45 % Fe (%wt) was designed as the substrate. It was polished with SiC papers (ranging from P320 to

P1200 grit), rinsed ultrasonic in distilled water for 15 minutes, then dried at room temperature and last limited the working area to 1 cm^2 by epoxy.

MgHAp coatings were synthesized on the 316L SS by cathodic scanning potential method in 80 mL solution containing Ca^{2+}, $H_2PO_4^-$, Na^+ and Mg^{2+}. The solutions were denoted as following:

SMg0: 3×10^{-2} M $Ca(NO_3)_2$ + 1.8×10^{-2} M $NH_4H_2PO_4$ + 6.0×10^{-2} M $NaNO_3$

SMg1: SMg0 + 1×10^{-4} M $Mg(NO_3)_2$

SMg2: SMg0 + 5×10^{-4} M $Mg(NO_3)_2$

SMg3: SMg0 + 1×10^{-3} M $Mg(NO_3)_2$

SMg4: SMg0 + 5×10^{-3} M $Mg(NO_3)_2$

MgHAp coatings were synthesized with the different scanning potential ranges of 0 to -1.5; 0 to -1.7; 0 to -1.9 and 0 to -2.1 V/SCE; different scanning times of 3; 4; 5; 6; 7 and 10 scans.

The electrodeposition was carried out in a three-electrode cell: 316L SS as the working electrode; platinum foil electrode acting as the counter electrode and a saturated calomel electrode (SCE) as the reference electrode on the Autolab PGSTAT 30 equipment (Holland).

2.2. Coating characterization

Mass of MgHAp coatings deposited on the surface of 316L SS was determined by the mass change of 316L SS samples before and after synthesis by a Precisa analytical balance (XR 205SM-PR, Swiss). Thickness of the coatings was measured by Alpha-Step IQ system (KLA-Tencor-USA), following the standard of ISO 4288-1998. The result is the average value of 5 measurements. The charge of synthesis process was determined by taking the integral from the start to the end point of the cathodic polarization curve. The adhesion strength of the coatings on 316L SS substrate was examined using an automatic adhesion tester (PosiTest AT-A, DeFelsko) according to ASTM D-4541 standard [9].

Fourier transform infrared (FTIR) spectra were recorded in the range of 4000-400 cm^{-1}, with a resolution of 8 cm^{-1} by a Nicolet 6700 Spectrometer, using the KBr pellet technique. The spectra were the sum of 32 scans. The morphology of the coatings was characterized using scanning electron microscopy (SEM) using Hitachi S4800 equipment (Japan). JSM 6490-JED 1300 Jeol (Japan) energy-dispersive X-ray spectroscopy (EDS) was used to identify the composition of elements in MgHAp coatings. The phase structure and crystallinity of the MgHAp coatings were analyzed by X-ray diffraction (SIEMENS D5005 Bruker-Germany, CuK_α radiation (λ = 1.54056 Å), with the following parameters: step angle of 0.03°, the scanning rate of 0.03 $°s^{-1}$, and 2θ in a range of 10-70°. The crystallite size of HAp and MgHAp was calculated from (002) reflection in XRD pattern, using Scherrer's equation [5].

Lattice parameters (a, c) were calculated from peak (002) and (211) of XRD pattern according to equation 1. Where, d is determined from XRD, which is the distance between adjacent planes in the set of Miller indices (hkl) [10]:

$$\frac{1}{d^2} = \frac{\frac{4}{3}(h^2 + kh + k^2)}{a^2} + \frac{l^2}{c^2} \quad (1)$$

3. RESULTS AND DISCUSSION

3.1. Effect of Mg^{2+} concentration

The cathodic polarization curves of 316L SS substrate in the electrolytes SMg0, SMg1, SMg2, SMg3 and SMg4 at 50 ^oC, 0÷-1.7 V/SCE, 5 scanning times are shown in Fig. 1. The concentration of Mg^{2+} in the electrolyte solution increase leading to improve the ionic strength of the electrolyte, so the current density increases.

With the potential range 0÷-0.6 V/SCE, the values of the current density are nearly unchanged and approximately zero because no reaction occurs on 316L SS substrate. With the potential is -0.6÷-1.2 V/SCE, the current density increased slightly due to the reduction of O_2 to produce OH^- [5].

When potential is more negative than -1.2 V/SCE, the current density increases fast because several electrochemical reactions occur, such as: the reduction: NO_3^-, $H_2PO_4^-$, H_2O to produce OH^-; PO_4^{3-} and H_2 [5, 7, 11].

Hydroxide is generated on the cathode surface to lead the formation PO_4^{3-} ions by acid-base reaction of $H_2PO_4^-$ and OH^- [5, 7].

Then MgHAp is producted on the cathode substrate according to the chemical reaction [5]:

$$10(Ca^{2+}, Na^+, Mg^{2+}) + 6PO_4^{3-} + 2OH^- \rightarrow (Ca,Na,Mg)_{10}(PO_4)_6(OH)_2 \quad (2)$$

Figure 2 shows the IR spectra in the wave number range from 4000 to 400 cm^{-1} of MgHAp coatings which were synthesized in SMg1, SMg2, SMg3 and SMg4 solutions. The results shows the characteristic peaks of HAp such as PO_4^{3-} and OH^-. The peaks of PO_4^{3-} group are observed at 1035; 602; 565 and 437 cm^{-1}; the vibrations of OH^- are observed at 3447 and 1645 cm^{-1}. Furthermore, the peaks of NO_3^- and CO_3^{2-} were also detected respectively at 1384 and 864 cm^{-1} because NO_3^- ions are present in the electrolyte; CO_2 from in the air can be dissolved in the electrolyte and reacts with OH^- to form the CO_3^{2-} ions [5, 7].

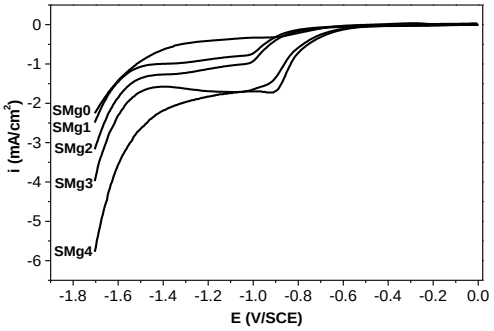

Figure 1: The cathodic polarization curve of 316L SS substrate in SMg0, SMg1, SMg2, SMg3 and SMg4 solution

The element components of obtained coatings were analyzed by the EDX spectra. The results showed the presence of 5 main elements in MgHAp coatings: O, P, Ca, Mg and Na. With the concentration of Mg^{2+} in the solution increased from 1×10^{-4} to 5×10^{-3} M, the content of Mg in MgHAp coatings increased from 0.06 to 0.4 wt% (table 1). These results have been used to calculate the atomic ratios M/Ca, (Ca+M)/P. The ratio of (Ca+0.5Na+Mg)/P and Na/Ca in all samples are lower than the ratio of Ca/P in the natural bone (1.67 and 0.102, respectively) [12, 13]. The deposited MgHAp coatings have the ratio Mg/Ca from 0.0057 to 0.0195. However, to reach the Mg/Ca ratio ≤ 0.017, similar to natural bone [12, 13], the obtained MgHAp coatings in the electrolyte solution SMg1, SMg2 and SMg3 are suitable. Therefore, SMg3 was chosen for the next experiments.

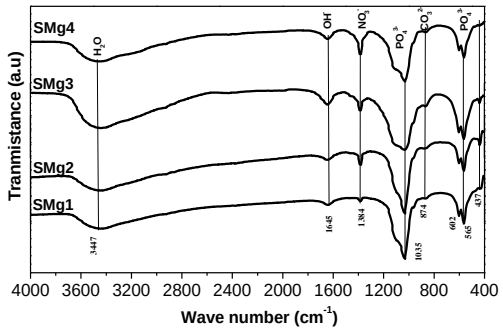

Figure 2: IR spectra of MgHAp coatings synthesized in the solutions: SMg1, SMg2, SMg3 and SMg4 at 50 ^{o}C, 0÷-1.7 V/SCE, 5 scans

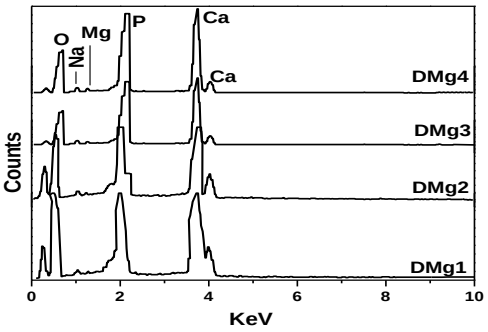

Figure 3: The EDX spectra of MgHAp coatings synthesized on 316L SS at 50 ^{o}C, 0÷-1.7 V/SCE, 5 scans in the electrolyte solutions: SMg1, SMg2, SMg3 and SMg4

Table 1: The component of elements of MgHAp synthesized on 316L SS in SMg1, SMg2, SMg3 and SMg4 solutions at 50 ^{o}C, 0÷-1.7 V/SCE, 5 scans

Electrolyte	% Mass					Na/Ca	Mg/Ca	(0.5 Na+Sr +Ca)/ P
	O	P	Ca	Na	Mg			
SMg1	47.43	17.18	34.12	1.21	0.06	0.062	0.0029	1.59
SMg2	45.65	17.90	35.20	1.13	0.12	0.056	0.0057	1.58
SMg3	45.90	18.10	34.60	1.20	0.20	0.060	0.0096	1.54
SMg4	45.80	18.50	34.20	1.10	0.40	0.056	0.0195	1.50

3.2. Effect of the scanning potential range

The influence of the scanning potential ranges on the deposition of MgHAp coatings was studied in the SMg3 solution. The charge, mass, thickness and adhesion strength of MgHAp coatings at the different potential ranges of 0÷-1.5, 0÷-1.7, 0÷ -1.9, and 0÷-2.1 V/SCE are shown in Table 2. The charge increases from 0.42 C to 6.85 C when the scanning potential range extends from 0÷-1.5 to 0÷-2.1 V/SCE. Therefore, according to Faraday law, OH^- and PO_4^{3-} ions are formed more so the mass of obtained coatings increases. However, the mass and thickness of MgHAp coatings increases and reaches the maximum value at potential range of 0÷-1.7 V/SCE (2.63 mg/cm^2 and 8.1 µm). With the more negative potential range, these values decrease. The results are explained that with the negative scanning potential range leading to the increase of the charge, further increase the amount of OH^- and PO_4^{3-} ions on the electrode surface leading to diffuse into the solution to form MgHAp. Moreover, with the more

negative potential range, the adhension strength between MgHAp coatings and 316L SS substrate decreases and the obtained coatings are porous because of the formation of hydrogen bubbles on the electrode surface. Thus, the potential range 0 to -1.7 V/SCE is chosen for the next experiments.

Table 2: The variation of charge, mass, thickness and adhesion strength of obtained coating at 50 ^{o}C, 5 scans in SMg3 solution with the different scanning potential ranges

Potential range (V/SCE)	Charge (C)	MgHAp mass (mg/cm^2)	Thickness (μm)	Adhesion strength (MPa)
0÷-1.5	0.42	1.21	5.5	7.32
0÷-1.7	3.56	2.63	8.1	7.20
0÷-1.9	4.52	1.96	6.3	7.10
0 ÷-2.1	6.85	1.41	4.5	6.95

3.3. Effect of the scanning times

Results of charge, mass, thickness and adhesions strength of obtained MgHAp coatings with the scanning times from 1 to 10 scans are shown in table 3. With one scanning time, the charge is 0.76 C, the adhesion strength reached the highest value (12.97 MPa). This value is nearly with the adhesion of glue and 316L SS (15 MPa). This is explained that because the mass and thickness of deposited MgHAp are small (0.57 mg/cm^2 and 1.6 μm), not enough to cover all surface of the substrate, so the obtained adhesion strength is contributed by the substrate and glue. The charge of deposited process increases according to scanning times. However, the mass and thickness of coatings only increase with scanning times increasing from 1 to 5 scans and then decrease. The adhesion strength decrease from 12.97 MPa to 5.72 MPa with scanning times increase from 1 to 10 scans. It is explained that the charge increases leading to OH^- and PO_4^{3-} ions forming too much on the electrode surface and diffusing into the solution so MgHAp is formed in the solution without sticking the substrate. Thus, 5 scanning time is chosen for MgHAp coating electrodeposition.

Table 3: The variation of the adhesion strength of MgHAp coatings to 316L SS in SMg3 at 50 ^{o}C, 0÷-1.7 V/SCE with different scanning times

Scanning times (times)	Charge (C)	MgHAp mass (mg/cm^2)	Thickness (μm)	Adhesion (MPa)
1	0.76	0.57	1.6	12.97
3	2.40	1.72	5.5	7.31
5	3.51	2.63	8.1	7.20
7	4.61	1.41	4.5	6.31
10	6.33	0.98	3.1	5.72

3.4. Characterization of MgHAp coating

*The XRD patterns

Figure 4 shows the XRD patterns of HAp and MgHAp coatings. Both XRD patterns exhibit the hydroxyapatite phase with two characteristic peaks at 2θ of 32 ^{o} (211) and 26 ^{o} (002). Besides, there are some peaks of HAp with smaller intensity at 2θ of 17^{o} (101), 33^{o} (300), 46^{o} (222), and 54^{o} (004). The characteristic peaks of 316L SS substrate are observed at 2θ ≈ 45^{o} (Fe) and ≈ 44^{o}, 51^{o} (CrO.19FeO.7NiO). These results show that MgHAp coatings have crystals structure and single phase of HAp.

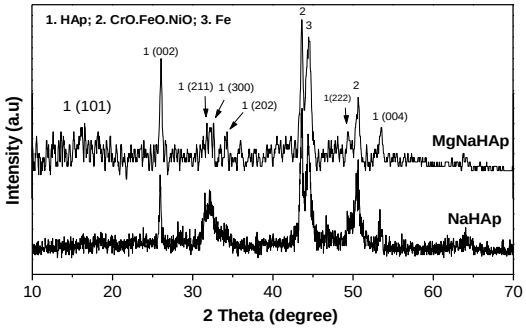

Figure 4: XRD patterns of HAp and MgHAp synthesized in SMg0 and SMg3 solution at 0÷-1.7 V/SCE, 50 ^{o}C, and 5 scans

The crystal diameters of HAp and MgHAp are calculated according to Scherrer formula (Equation 2). The crystal diameter of MgHAp coating is about 22.1 nm, smaller than that of HAp (44.2 nm). This can be explained that the radius of Mg^{2+} ion (0.65 Å) is smaller than Ca^{2+} (0.99 Å) and Na^{+} (0.95 Å) so Ca^{2+}, Na^{+} are replaced by Mg^{2+} leading to reduce the crystal diameter.

Table 4 presents distance between the adjacent planes of the crystal (d) at two planes (002) and (211) and the value of the lattice parameters a, b, c of MgHAp. In comparison with NIST standard of HAp sample [10] and HAp, these values of MgHAp is lower. This result shows that Mg^{2+}, Na^{+} ions incorporated into the HAp lattice structure.

Table 4: Values of distance between the planes of the crystal and the lattice constant of MgHAp and HAp

	HAp [10]	HAp	MgHAp
d (002)	3.44	3.438	3.420
d (211)	2.82	2.815	2.768
a = b (Å)	9.4451	9.4261	9.247
c (Å)	6.88	6.876	6.840

*** SEM images**

SEM images of HAp and MgHAp coating synthesized on 316L SS were presented in Fig. 5. The results showed that with the present of Mg, the morphology changes from plate shapes of HAp to fibrous shapes of MgHAp.

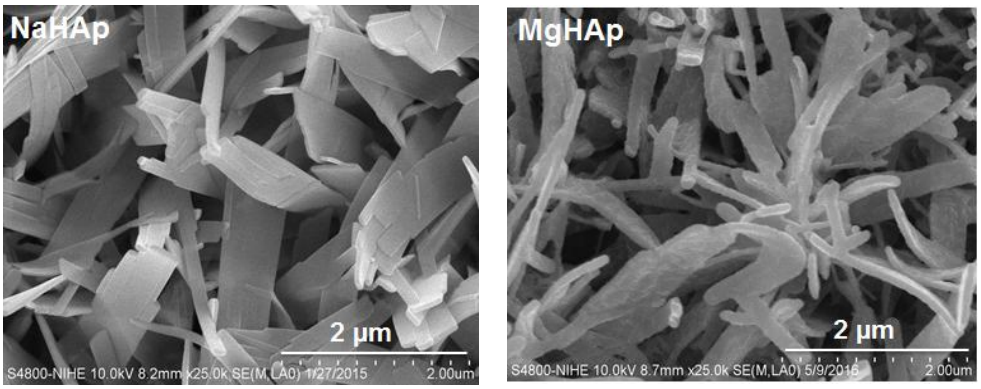

Figure 5: The SEM images of HAp and MgHAp coatings deposited in SMg0 and SMg3 solutions, at 50 ^{o}C, 0÷-1.7 V/SCE, 5 scans

4. CONCLUSION

MgHAp coatings have been successfully synthesized on 316L SS substrate by the electrodeposition method. The optimal conditions were chosen to deposite MgHAp coatings. The obtained MgHAp has single phase crystals of HAp, fibrous shape and the content of 0.2 wt% Mg and 1.2 wt% Na similar to natural bone which could be improved mechanical properties and biological activity of HAp. With these good characteristics, MgHAp coatings would be applied to produce good implant materials.

REFERENCES

1. Xin Fan, Jian Chen, Jian-Peng Zou, Qian Wan, Zhong-Cheng Zhou, Jian-Ming Ruan. *Bone-like apatite formation on HA/316L stainless steel composite surface in simulated body fluid*, Transactions of Nonferrous Metals Society of China, **19**(2), 347-352 (2009).
2. Piña Barba, Guzmán Vázquez, Munguia. *Stoichiometric Hydroxyapatite Obtained by Precipitation and Sol-Gel Processes,* Revista Mexicana de Fisica, **51(3)**, 284-293 (2005).
3. A. Dey, A. K. Mukhopadhyay, S. Gangadharan, M. K. Sinha, D. Basu, N. R. Bandyopadhyay. *Nanoindentation study of microplasma sprayed hydroxyapatite coating,* Ceramics International, **35(6)**, 2295-2304 (2009).
4. T. M. Sridhar N.Eliaz, U. Kamachi Mudali and Baldev Raj. *Electrochemical and electrophoretic deposition of hydroxyapatite for orthopaedic applications,* Surface Engineering, **21(3)**, 238-242 (2005).
5. Pham Thi Nam, Dinh Thi Mai Thanh, Nguyen Thu Phuong, Le Xuan Que, Nguyen Van Anh, Thai Hoang, Tran Dai Lam. *Controlling the electrodeposition, morphology and structure of hydroxyapatite coating on 316L stainless steel,* Materials Science and Engineering, **C 33(4)**, 2037-2045 (2013).
6. Zhang Leilei, Li Hejun, Li Kezhi, Zhang Shouyang, Fu Qiangang, Zhang Yulei, Lu Jinhua, Li Wei, *Preparation and characterization of carbon/SiC nanowire/Na-doped carbonated hydroxyapatite multilayer coating for carbon/carbon composites,* Applied Surface Science, **313(0)**, 85-92 (2014).

7. Qiongqiong Dinga, Yajing Yan, Yong Huang, Shuguang Hana, Xiaofeng Pang. *Magnesium substituted hydroxyapatite coating on titanium with nanotublar TiO_2 intermediate layer via electrochemical deposition*, Applied Surface Science, **305**, 77-85 (2014).
8. A. Sharifnabi, M. H. Fathi, B. Eftekhari Yekta, M. Hossainalipour. *The structural and bio-corrosion barrier performance of Mg-substituted fluorapatite coating on 316L stainless steel human body implant*, Applied Surface Science, **288**, 331-340 (2014).
9. Standard Test Method for Pull-Off Strength of Coating Using Portable Adhension Testers Astm D-4541, Annual Book of ASTM Standards, American Society for Testing and Materials, Philadelphia, Pa, USA (2002).
10. Standard Reference Material 2910. Calcium Hydroxyapatite. Institute of Standards and Technology, Nist Measurement Services Division National (2008).
11. Jian Wang, Yonglie Chao, Qianbing Wan, Zhimin Zhu, Haiyang Yu. *Fluoridated hydroxyapatite coatings on titanium obtained by electrochemical deposition*, Acta Biomaterialia, **5(5)**, 1798-1807 (2009).
12. H. J. M. Bowen. *Environmental Chemistry of the Element*, London: Academic Press, Inc 1979.
13. U. H. -W. Kuoa, S. -M. Kuoa, C. -H. Choub, T. -C. Leeb. *Determination of 14 elements in Taiwanese bones*, The Science of the Total Environment, **25**, 45-54 (2000).

Corresponding author: **Vo Thi Hanh**
Department of Chemistry, Basic Science Faculty
Hanoi University of Mining and Geology
E-mail: vothihanh2512@gmail.com; Telephone 0982541229.